Design Simulations of the SJTU Continuum Arm Exoskeleton (SCAX)

Kai Xu, You Wang, and Dong Qiu

RII Lab (Lab of Robotics Innovation and Intervention), UM-SJTU Joint Institute,
Shanghai Jiao Tong University, Shanghai, 200240, China
{k.xu,youwang,d.qiu}@sjtu.edu.cn

Abstract. In a clinical environment for rehabilitation therapy, one exoskeleton is usually shared by multiple patients. If the exoskeleton has a rigid structure which is actuated to mobilize a patient, it will be challenging to guarantee these on-site adjustments can make the rigid exoskeleton fit each patient kinematically perfectly. This paper proposes to design an exoskeleton using compliant continuum mechanisms. Its intrinsic flexibility allows the adaption to different human anatomies passively. The design concept, kinematics and design simulations are elaborated for this SJTU Continuum Arm Exoskeleton (SCAX). Combining previous experimental results for a proof-of-concept shoulder exoskeleton, the SCAX could effectively achieve consistent Anatomy Adaptive Assistances (AAA) for different patients with their limb motions.

Keywords: Exoskeleton, continuum mechanisms, kinematics, SCAX (SJTU Continuum Arm Exoskeleton), AAA (Anatomy Adaptive Assistances).

1 Introduction

Research on exoskeletons has been quite active in the past decades. Numerous exoskeleton systems were developed for upper and lower limbs for military and medical applications (e.g. [1, 2]). These exoskeleton systems either aim to augment a healthy wearer's physical performance with robotic actuation or to deliver rehabilitation therapies to patients with neuromuscular defects after stroke or injury. Examples include the performance-augmenting exoskeleton from UC Berkeley [3], the load-carrying exoskeleton from MIT [4], rehabilitation exoskeletons for lower limbs [5-9], and those for upper limbs [10-17]. Actuation schemes of these systems include hydraulic cylinders [3] or pneumatic cylinders [5, 15, 18], pneumatic muscle actuators [10], cables [7, 11, 17], parallel mechanisms [8, 12, 14], gearmotors [19] and so on.

Besides these systems, research was also about enabling technologies, such as inertia compensation [20], sensing & control [4, 21-24], and most importantly ergonomics [25-27].

Many of the existing exoskeleton systems shared one similar design methodology: an articulated rigid kinematic chain is actuated to move an attached wearer. The use of rigid mechanisms in an exoskeleton might be suitable for applications for strength augmentation so that excessive external loads can be undertaken so as to shield the

J. Lee et al. (Eds.): ICIRA 2013, Part I, LNAI 8102, pp. 351–362, 2013.

wearer. But the use of rigid mechanisms introduces drawbacks such as bulkiness, high inertia, and most importantly the difficulty of maintaining kinematic compatibility between the exoskeleton and a human anatomy. In a clinical environment for rehabilitation therapy, one exoskeleton is usually shared by a group of patients. If the exoskeleton has a rigid structure, it will be challenging to guarantee these on-site adjustments can make the rigid exoskeleton fit each patient kinematically perfectly. Hence, design possibilities of using compliant components could be investigated. These attempts include a simulation work that used elastic cords to assist walking [28], an upper body exoskeleton using pneumatic artificial muscles [29], a cable-driven upper-limb exoskeleton [16, 17], and a proof-of concept continuum shoulder exoskeleton [30-32].

This paper presents the design concept, kinematics and simulation verifications of the SJTU Continuum Arm Exoskeleton (SCAX) as shown in Fig. 1. The contribution of this paper is mainly the proposal of designing an arm exoskeleton for rehabilitation using continuum mechanisms. Intrinsic compliance of such a continuum exoskeleton adapts to different human anatomies passively and can always assure the kinematic compatibility between itself and a group of patients.

The paper is organized as follows. Section 2 presents the design concept. Section 3 presents nomenclature and kinematics so that the simulation verifications can be presented in Section 4. Conclusions and future work are summarized in Section 5.

2 Design Concept

The continuum shoulder exoskeleton as in Fig. 1 consists of i) a rigid forearm sleeve, ii) a flexible elbow brace, iii) a rigid upper arm sleeve, iv) a flexible shoulder brace, v) a body vest, vi) a set of guiding cannulae, and vii) an actuation unit. Actuation of the continuum elbow brace and the continuum shoulder brace orients a patient's arm accordingly. This work is inspired by the designs from [33-35] where downscaled such continuum structures were used in surgical robots.

Structures of the continuum elbow brace and the continuum shoulder brace are similar. A schematic structure is also depicted in Fig. 2. Each brace consists of an end ring, a base ring, a few spacer rings and several secondary backbones. All the backbones are made from thin NiTi (Nickel-Titanium alloy) rods.

For either the shoulder brace or the elbow brace, the secondary backbones are only attached to the end ring and can slide in holes of the spacer rings and the base ring. The backbones for the elbow brace are routed through the upper arm sleeve and the shoulder brace. The backbones for the elbow and the shoulder braces are all routed through the set of guiding cannulae to the actuation unit, which simultaneously pulls and pushes these backbones to bend the continuum braces to orient a patient's upper arm and forearm. Miniature springs are used to keep the spacer rings evenly distributed to prevent buckling of the secondary backbones.

Advantages of the continuum exoskeleton include: i) safety and comfort introduced by the inherent compliance, ii) passive adaptation to different patient anatomies, iii) size scalability, iv) a redundant backbone arrangement for load redistribution and reduced buckling risks, and v) design compactness achieved by dual roles of these backbones as both the structural components and the motion output members.

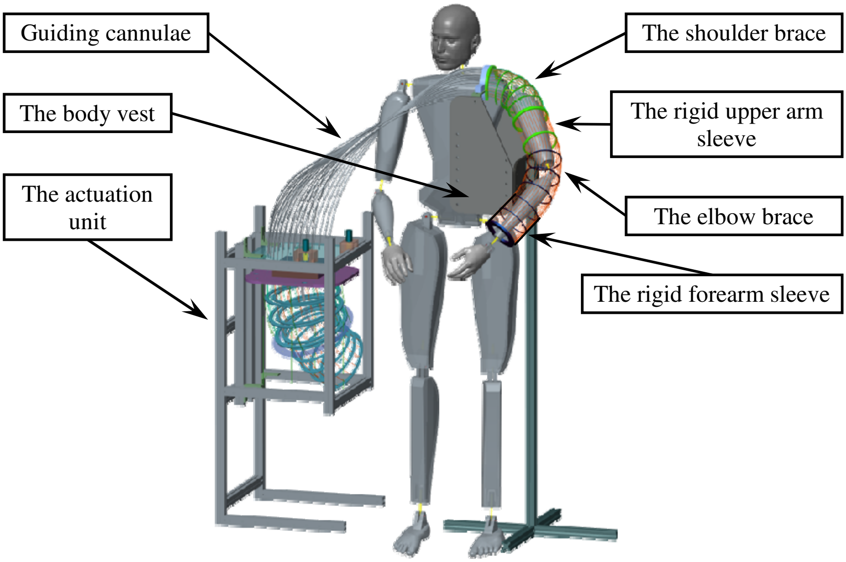

Fig. 1. Design concept of the SJTU Continuum Arm Exoskeleton (SCAX)

3 Nomenclature and Kinematics

The nomenclature and the kinematics assume that the continuum braces (the shoulder and the elbow braces) bend into a planar shape within the bending plane as shown in Fig. 2. Shapes of the secondary backbones are assumed by a sweeping motion of the structure's cross section along the primary backbone. The cross section is assumed rigid and perpendicular to the primary backbone. Different from previously published results [34, 36, 37], this work doesn't assume shape of the imaginary primary backbone to be circular, which has been experimentally verified in [31].

3.1 Nomenclature and Coordinate Systems

Since the shoulder brace and the elbow brace are structurally similar, the structure in Fig 2 could be applied as the shoulder brace or the elbow brace with different arrangement of the backbones.

To describe the structure, nomenclatures are defined in Table I, while coordinate systems of the continuum brace are defined as below

- *Base Ring Coordinate System* (BRS) is designated as $\{tb\} \equiv \{\hat{\mathbf{x}}_{tb}, \hat{\mathbf{y}}_{tb}, \hat{\mathbf{z}}_{tb}\}$. It is attached to the base ring of the continuum brace, whose XY plane coincides with the base ring and its origin is at the center of the base disk. $\hat{\mathbf{x}}_{tb}$ points from the center of the base disk to the first secondary backbone while $\hat{\mathbf{z}}_{tb}$ is perpendicular to the base ring. The secondary backbones are numbered according to the definition of δ_i.

- *Bending Plane Coordinate System 1* (BPS1) is designated as $\{t1\} \equiv \{\hat{\mathbf{x}}_{t1}, \hat{\mathbf{y}}_{t1}, \hat{\mathbf{z}}_{t1}\}$ which shares its origin with $\{tb\}$ and has the brace bending in its XZ plane.
- *Bending Plane Coordinate System 2* (BPS2) is designated as $\{t2\} \equiv \{\hat{\mathbf{x}}_{t2}, \hat{\mathbf{y}}_{t2}, \hat{\mathbf{z}}_{t2}\}$ obtained from $\{t1\}$ by a rotation about $\hat{\mathbf{y}}_{t1}$ such that $\hat{\mathbf{z}}_{t1}$ becomes backbone tangent at the end ring. Origin of $\{t2\}$ is at center of the end ring.
- *End Ring Coordinate System* (ERS) $\{te\} \equiv \{\hat{\mathbf{x}}_{te}, \hat{\mathbf{y}}_{te}, \hat{\mathbf{z}}_{te}\}$ is fixed to the end ring. $\hat{\mathbf{x}}_{te}$ points from center of the end ring to the first secondary backbone and $\hat{\mathbf{z}}_{te}$ is normal to the end ring. $\{te\}$ is obtained from $\{t2\}$ by a rotation about $\hat{\mathbf{z}}_{t2}$.

Table 1. Nomenclature used in this paper

t	Index of the continuum braces: $t = 1$ for the shoulder brace and $t = 2$ for the elbow brace
m	Index of the secondary backbones, $i = 1, 2, \cdots, m$
r_{ti}	In the indicated brace, distance from the imaginary primary backbone to the *ith* secondary backbone. r_{ti} can be different for different t and i.
β_{ti}	In the indicated brace, β_{ti} characterizes the division angle from the *ith* secondary backbone to the first secondary backbone. $\beta_{ti} \equiv 0$ and β_{ti} remain constant once the braces are built.
L_t, L_{ti}	In the indicated brace, lengths of the imaginary primary and the *ith* secondary backbones measured from the base ring to the end ring.
$\rho_t(s)$, $\rho_{ti}(s_{ti})$	In the indicated brace, radius of curvature of the primary and the *ith* secondary backbones.
$\mathbf{q}_t$	In the indicated brace, $\mathbf{q}_t = [q_{t1} \;\; q_{t2} \;\; \cdots \;\; q_{tm}]^T$ is the actuation lengths for the secondary backbones and $q_{ti} \equiv L_{ti} - L_t$.
$\theta_t(s)$	In the indicated brace, angle of the tangent to the imaginary primary backbone in the bending plane. $\theta_t(L)$ and $\theta_t(0)$ are designated by θ_{tL} and θ_0, respectively. $\theta_0 = \pi/2$
δ_{ti}	In the indicated brace, a right-handed rotation angle about $\hat{\mathbf{z}}_{t1}$ from $\hat{\mathbf{x}}_{t1}$ to a ray passing through the imaginary primary backbone and the *ith* secondary backbone.
δ_t	$\delta_t \equiv \delta_{t1}$ and $\delta_{ti} = \delta_t + \beta_{ti}$
$\boldsymbol{\psi}_t$	$\boldsymbol{\psi}_t \equiv [\theta_{tL} \;\; \delta_t]^T$ defines the configuration of the indicated brace.
${}^{tb}\mathbf{p}_t(s)$	In the indicated brace, position vector of a point along the primary backbone in $\{tb\}$. ${}^{tb}\mathbf{p}_t(L)$ is the tip position and is designated by ${}^{tb}\mathbf{p}_{tL}$.

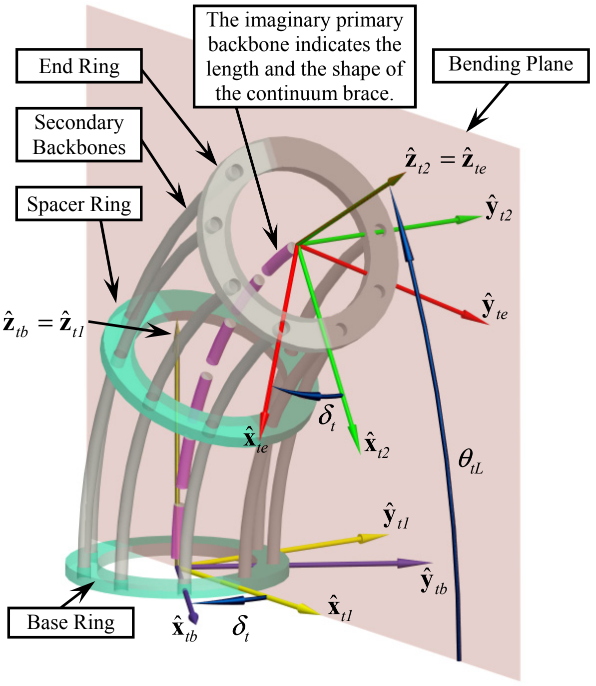

Fig. 2. Nomenclature and coordinates of the continuum brace

3.2 Kinematics

Thorough kinematics analysis of such a continuum brace can be found in [34, 36, 37]. This work here emphasizes the shape of the primary backbone to be non-circular (the result also applies if the shape is circular) and arrangements of the secondary backbones to be arbitrary (assigning different values to r_{ti} and β_{ti}).

Configuration of the continuum brace is parameterized by $\boldsymbol{\psi}_t = \begin{bmatrix} \theta_{tL} & \delta_t \end{bmatrix}^T$. Since shapes of the secondary backbones are assumed by a sweeping motion of the structure's cross section along the primary backbone, projection of the i*th* secondary backbone on the bending plane is a curve which is offset by Δ_{ti} from the primary backbone. Its radius of curvature and arc-length are indicated by $\rho_{ti}(s_{ti})$ and s_{ti}. They are related to the parameters of the primary backbone as follows:

$$\rho_t(s) = \rho_{ti}(s_{ti}) + \Delta_{ti} \quad . \tag{1}$$

Where $\Delta_{ti} \equiv r_{ti} \cos \delta_{ti}$

The length of the primary backbone and the length of the i*th* backbone are related according to:

$$L_{ti} = \int ds_{ti} = \int \left(ds_{ti} - ds_t + ds_t \right) = \int \left(ds_{ti} - ds_t \right) + L_t \quad . \tag{2}$$

The integral above can be rewritten as in Eq. (3). Substituting Eq. (1) into Eq. (3) gives Eq.(4), which leads to the result as in Eq. (5):

$$\int \left(ds_{ti} - ds_t \right) = \int_0^{\theta_0 - \theta_{tL}} \left(\rho_{ti}\left(s_{ti}\right) - \rho_t\left(s_t\right) \right) d\theta \quad . \tag{3}$$

$$\int_0^{\theta_0 - \theta_{tL}} \left(\rho_{ti}\left(s_{ti}\right) - \rho_t\left(s_t\right) \right) d\theta = - \int_0^{\theta_0 - \theta_{tL}} \Delta_{ti} d\theta \quad . \tag{4}$$

$$L_{ti} = L_t - r_{ti} \cos\delta_{ti} \left(\theta_0 - \theta_{tL} \right) = L_t + r_{ti} \cos\delta_{ti} \left(\theta_{tL} - \theta_0 \right) \quad . \tag{5}$$

Referring to the definition of q_{ti} in Table 1, Eq. (5) gives:

$$q_{ti} = r_{ti} \cos\delta_{ti} \left(\theta_{tL} - \theta_0 \right), \ i = 1, 2, \cdots, m \quad . \tag{6}$$

Equation (6) states that actuation of this continuum brace only depends on the values of θ_{tL} and δ_t, no matter what the actual shape of the primary backbone is. This characteristics provides a particular advantage: when the brace is put on different patients, different anatomies give different shapes of the primary backbone, but the actuation remains the same while orienting the limb to the same direction (the direction is characterized by θ_{tL} and δ_t).

Rotation matrix ${}^{b}\mathbf{R}_{e}$ associates $\{te\}$ and $\{tb\}$:

$${}^{tb}\mathbf{R}_{te} = \mathrm{R}\left(\hat{\mathbf{z}}_{tb}, -\delta_t \right) \mathrm{R}\left(\hat{\mathbf{y}}_{t1}, \theta_0 - \theta_{tL} \right) \mathrm{R}\left(\hat{\mathbf{z}}_{t2}, \delta_t \right) \quad . \tag{7}$$

Where $\mathrm{R}\left(\hat{\mathbf{n}}, \gamma \right)$ represents rotation about $\hat{\mathbf{n}}$ by an angle γ.

Tip position of the continuum brace is given by:

$${}^{tb}\mathbf{p}_{tL} = {}^{tb}\mathbf{R}_{t1} \begin{bmatrix} \int_0^{L_t} \cos\left(\theta_t\left(s_t\right) \right) ds_t & 0 & \int_0^{L_t} \sin\left(\theta_t\left(s_t\right) \right) ds_t \end{bmatrix}^T \quad . \tag{8}$$

Where ${}^{tb}\mathbf{R}_{t1} = \mathrm{R}\left(\hat{\mathbf{z}}_{tb}, -\delta_t \right)$ and the integrals depend on the actual shape of the primary backbone.

4 Design Simulations

Actual shapes of the shoulder and the elbow braces depend on a minimal of the total potential energy of the exoskeleton-arm system (elastic potential energy of the continuum exoskeleton and the gravitational potential energy of the arm). The shapes would also be affected by the anatomical parameters (such as shoulder widths and arm lengths) of a patient.

Demonstrated experimentally as in [31], the shapes of the braces' secondary backbones were different from circular arcs. In fact the actual shapes kept changing during the motions of assisting a patient's limb. In order to verify the kinematics of the SCAX exoskeleton, the simulations are conducted with an assumption that the shape of one secondary backbone within the braces could be characterized as one circular arc plus a straight line, as shown in Fig. 3.

The arm in Fig. 3 consist of a shoulder joint, an upper arm, an elbow joint and a forearm with hand. The shoulder joint is represented by a spherical joint whereas the elbow joint is represented by a revolute joint.

The axis of the upper arm is aligned with $\hat{\mathbf{z}}_{1e}$ and the axis of the forearm is aligned with $\hat{\mathbf{z}}_{2e}$. Since the wearer's hand can be considered rigidly attached to the forearm sleeve, the position and the orientation of the hand can be characterized by ${}^{1b}\mathbf{p}_{hand}$ and ${}^{1b}\mathbf{R}_{2e}$ respectively as follows:

$$ {}^{1b}\mathbf{p}_{hand} = {}^{1b}\mathbf{p}_{1L} + {}^{1b}\mathbf{R}_{1e}\left\{ {}^{1e}\mathbf{p}_{\{1e\}\{2b\}} + {}^{2b}\mathbf{R}_{2e}\,{}^{2e}\mathbf{p}_{hand} \right\} \quad . \tag{9} $$

Where ${}^{2e}\mathbf{p}_{hand}$ is an arbitrary point within the hand described in $\{2e\}$ and ${}^{1e}\mathbf{p}_{\{1e\}\{2b\}}$ is the position vector from the origin of $\{1e\}$ to the origin of $\{2b\}$.

$$ {}^{1b}\mathbf{R}_{2e} = {}^{1b}\mathbf{R}_{1e}\,{}^{2b}\mathbf{R}_{2e} \quad . \tag{10} $$

Once the arm exoskeleton is built, lengths of the continuum braces and the sleeves will be kept constant. Structural parameters of the SCAX exoskeleton are listed in Table 2. L_{1s} and L_{2s} are the lengths of the upper arm sleeve and the forearm sleeve respectively.

Motion simulations were conducted for the four poses with the following configuration variables as shown in Fig. 4.

- ✧ $[\theta_{1L} = \pi/2 \;\; \delta_1 = 0 \;\; \theta_{2L} = \pi/2 \;\; \delta_2 = 0]^T$
- ✧ $[\theta_{1L} = \pi/3 \;\; \delta_1 = 3\pi/4 \;\; \theta_{2L} = \pi/2 \;\; \delta_2 = 0]^T$
- ✧ $[\theta_{1L} = \pi/6 \;\; \delta_1 = 3\pi/4 \;\; \theta_{2L} = \pi/2 \;\; \delta_2 = 0]^T$
- ✧ $[\theta_{1L} = \pi/6 \;\; \delta_1 = 3\pi/4 \;\; \theta_{2L} = \pi/3 \;\; \delta_2 = 3\pi/4]^T$

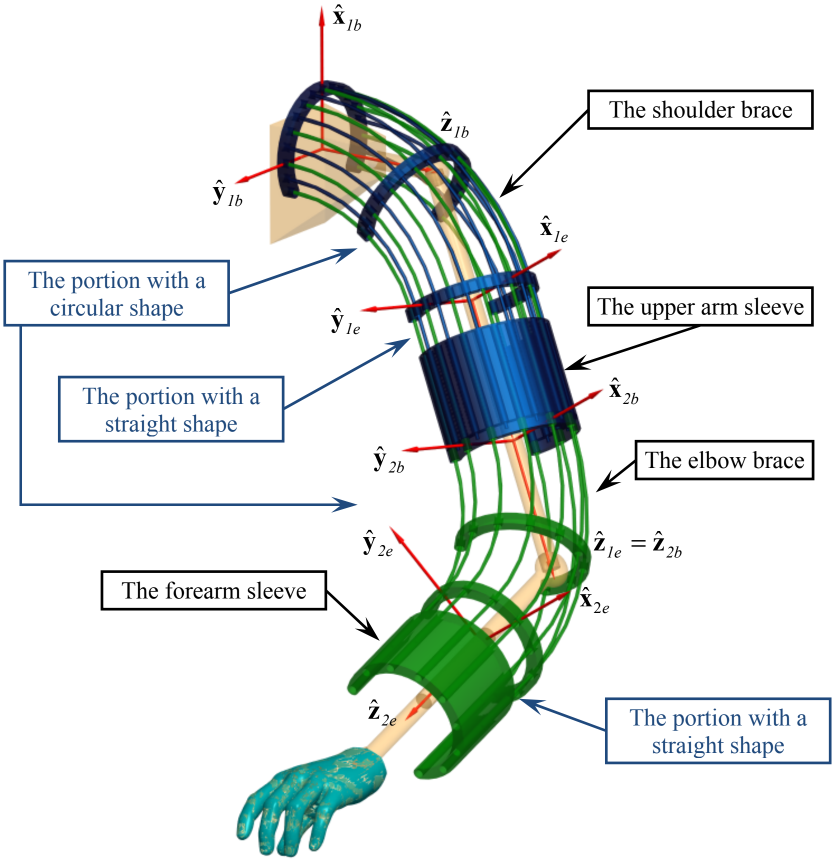

Fig. 3. Coordinate assignments of the SCAX exoskeleton

Table 2. Structural parameters of the SCAX exoskeleton

$L_1 = 280mm$	$r_{1i} = 65mm$	$L_{1s} = 80mm$	
$L_2 = 260mm$	$r_{2i} = 65mm$	$L_{2s} = 80mm$	
$\theta_{1L} \in [0\ \ \pi/2]^T$	$\delta_1 \in [-\pi\ \ \pi]^T$	$\theta_{2L} \in [0\ \ \pi/2]^T$	$\delta_2 \in [-\pi\ \ \pi]^T$

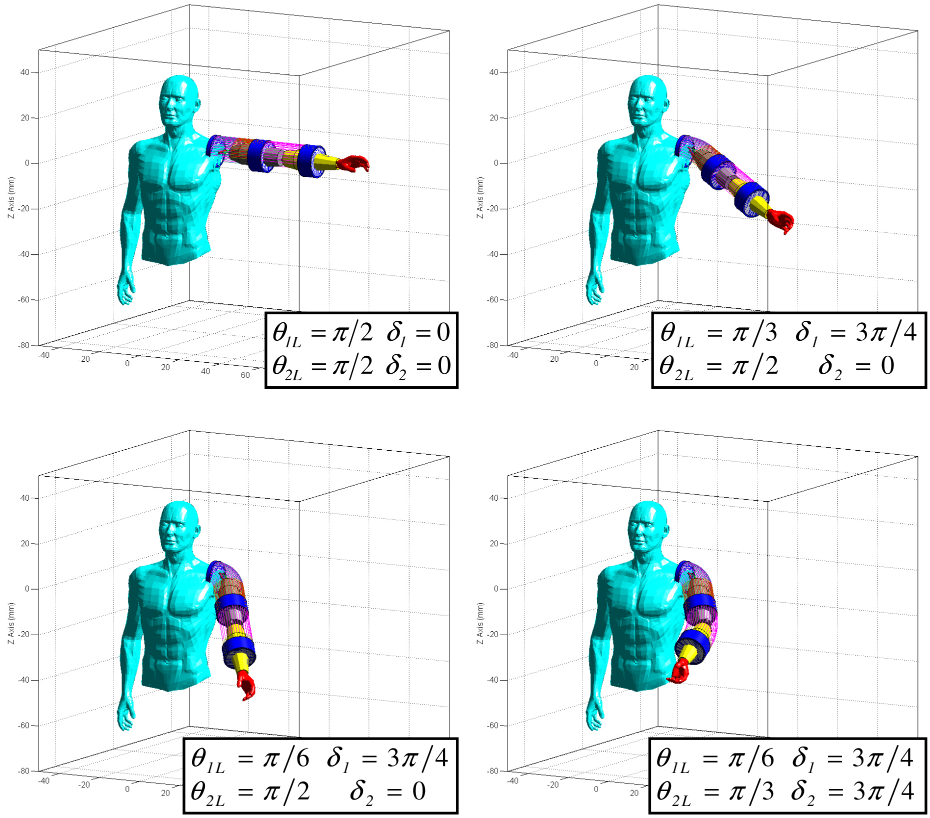

Fig. 4. Motion simulations of the SCAX exoskeleton

5 Conclusions and Future Work

This paper presented the design concept, kinematics and motion simulations of the SJTU Continuum Arm Exoskeleton (SCAX) which utilizes continuum braces to orient a patient wearer's arm for rehabilitation therapies. The secondary backbones in the continuum braces were pushed and pulled to achieve the actuation so as to assist a patient with upper arm motions.

During the assisted motions, the continuum braces in the exoskeleton were deformed and they passively adapted to different anatomies because of the intrinsic flexibility. Although shapes of the exoskeleton were different for different anatomies, the same actuation was able to assist the anatomically different arms with similar motions. This is a particular advantage for the exoskeleton's application in a clinical setting. When the exoskeleton is shared by a group of patients, without performing any hardware adjustments, the exoskeleton can match each patient's anatomy passively and assist his/her arm motions.

No firm attachment between the arm sleeves and the arm is needed. When the arm sleeves are oriented by the shoulder brace and the elbow brace, the arm rests in the sleeves naturally, preventing the exoskeleton from exerting excessive forces on the shoulder joint and on the elbow joint. In other words, the proposed design could potentially provide safe and effective rehabilitation to a group of anatomically different patients in an operation-friendly manner, where is hence referred as to a rehabilitation with Anatomy Adaptive Assistances (AAA rehabilitation).

Based on a general framework of the kinematics of the continuum braces, motion simulations were conducted to verify the motion capabilities of the SCAX exoskeleton while assisting an arm.

Future work mainly lies on two aspects. The first aspect is to design an effective and compact actuation unit to drive the shoulder and the elbow braces. The second aspect is to improve the ergonomics so that it can be used by impaired subjects. A possible solution is to design the continuum braces as two separable pieces which can be quickly assembled while putting on a patient. In this way the exoskeleton can also be conveniently peeled off when a therapeutic session is finished.

Acknowledgments. This work was supported in part by the National Program on Key Basic Research Projects (the 973 Program) #2011CB013300, and in part by Program for New Century Excellent Talents in University (the NCET Program).

References

1. Brewer, B.R., McDowell, S.K., Worthen-Chaudhari, L.C.: Poststroke Upper Extremity Rehabilitation: A Review of Robotic Systems and Clinical Results. Topics in Stroke Rehabilitation 14(6), 22–44 (2007)
2. Dollar, A.M., Herr, H.: Lower Extremity Exoskeletons and Active Orthoses: Challenges and State-of-the-Art. IEEE Transactions on Robotics 24(1), 144–158 (2008)
3. Zoss, A.B., Kazerooni, H., Chu, A.: Biomechanical Design of the Berkeley Extremity Exoskeleton (BLEEX). IEEE/ASME Transaction on Mechatronics 11(2), 128–138 (2006)
4. Walsh, C.J., Paluska, D., Pasch, K., Grand, W., Valiente, A., Herr, H.: Development of a Lightweight, Underactuated Exoskeleton for Load-Carrying Augmentation. In: IEEE International Conference on Robotics and Automation (ICRA), Orlando, Florida, USA (2006)
5. Durfee, W.K., Rivard, A.: Priliminary Design and Simulation of a Pneumatic, Stored-Energy, Hybrid Orthosis for Gait Restoration. In: ASME International Mechanical Engineering Congress, Anaheim, California, USA, pp. 1–7 (2004)
6. Banala, S.K., Agrawal, S.K., Fattah, A., Krishnamoorthy, V., Hsu, W.-L., Scholz, J., Rudolph, K.: Gravity-Balancing Leg Orthosis and Its Performance Evaluation. IEEE Transactions on Robotics 22(6), 1228–1239 (2006)
7. Veneman, J.F., Ekkelenkamp, R., Kruidhof, R., van der Helm, F.C.T., van der Kooij, H.: A Series Elastic- and Bowden-Cable-Based Actuation System for Use as Torque Actuator in Exoskeleton-Type Robots. International Journal of Robotics Research 25(3), 261–281 (2006)

8. Saglia, J.A., Tsagarakis, N.G., Dai, J.S., Caldwell, D.G.: A High Performance 2-dof Over-Actuated Parallel Mechanism for Ankle Rehabilitation. In: IEEE International Conference on Robotics and Automation (ICRA), Kobe, Japan, pp. 2180–2186 (2009)
9. Farris, R.J., Quintero, H.A., Goldfarb, M.: Preliminary Evaluation of a Powered Lower Limb Orthosis to Aid Walking in Paraplegic Individuals. IEEE Transactions on Neural Systems and Rehabilitation Engineering 19(6), 652–659 (2011)
10. Tsagarakis, N.G., Caldwell, D.G.: Development and Control of a 'Soft-Actuated' Exoskeleton for Use in Physiotherapy and Training. Autonomous Robots 15(1), 21–33 (2003)
11. Perry, J.C., Rosen, J., Burns, S.: Upper-Limb Powered Exoskeleton Design. IEEE/ASME Transaction on Mechatronics 12(4), 408–417 (2007)
12. Gupta, A., O'Malley, M.K., Patoglu, V., Burgar, C.: Design, Control and Performance of RiceWrist: A Force Feedback Wrist Exoskeleton for Rehabilitation and Training. International Journal of Robotics Research 27(2), 233–251 (2008)
13. Stienen, A.H.A., Hekman, E.E.G., Prange, G.B., Jannink, M.J.A., Aalsma, A.M.M., van der Helm, F.C.T., van der Kooij, H.: Dampace: Design of an Exoskeleton for Force-Coordination Training in Upper-Extremity Rehabilitation. Journal of Medical Devices 3(031003), 1–10 (2009)
14. Klein, J., Spencer, S., Allington, J., Bobrow, J.E., Reinkensmeyer, D.J.: Optimization of a Parallel Shoulder Mechanism to Achieve a High-Force, Low-Mass, Robotic-Arm Exoskeleton. IEEE Transactions on Robotics 26(4), 710–715 (2010)
15. Wolbrecht, E.T., Reinkensmeyer, D.J., Bobrow, J.E.: Pneumatic Control of Robots for Rehabilitation. International Journal of Robotics Research 29(1), 23–38 (2010)
16. Agrawal, S.K., Dubey, V.N., Gangloff, J.J., Brackbill, E., Mao, Y., Sangwan, V.: Design and Optimization of a Cable Driven Upper Arm Exoskeleton. Journal of Medical Devices 3(031004), 1–8 (2009)
17. Mao, Y., Agrawal, S.K.: Design of a Cable-Driven Arm Exoskeleton (CAREX) for Neural Rehabilitation. IEEE Transactions on Robotics 28(4), 922–931 (2012)
18. Vukobratovic, M., Hristic, D., Stojiljkovic, Z.: Development of Active Anthropomorphic Exoskeletons. Medical and Biological Engineering and Computing 12(1), 66–80 (1974)
19. Loureiro, R.C.V., Harwin, W.S.: Reach & Grasp Therapy: Design and Control of a 9-DOF Robotic Neuro-rehabilitation System. In: IEEE International Conference on Rehabilitation Robotics (ICORR), Noordwijk, The Netherlands, pp. 757–763 (2007)
20. Aguirre-Ollinger, G., Colgate, J.E., Peshkin, M.A., Goswami, A.: Design of an Active One-Degree-of-Freedom Lower-Limb Exoskeleton with Inertia Compensation. International Journal of Robotics Research (2010) (onlinefirst)
21. Kawamoto, H., Lee, S., Kanbe, S., Sankai, Y.: Power Assist Method for HAL-3 using EMG-based Feedback Controller. In: IEEE International Conference on Systems, Man and Cybernetics (IEEE SMC), Washington, D.C, USA, pp. 1648–1653 (2003)
22. Yamamoto, K., Ishii, M., Noborisaka, H., Hyodo, K.: Stand Alone Wearable Power Assisting Suit: Sensing and Control Systems. In: IEEE International Workshop on Robot and Human Interactive Communication, Kurashiki, Okayama, Japan (2004)
23. Fleischer, C., Hommel, G.: A Human–Exoskeleton Interface Utilizing Electromyography. IEEE Transactions on Robotics 24(4), 872–882 (2008)
24. Sharma, V., McCreery, D.B., Han, M., Pikov, V.: Bidirectional Telemetry Controller for Neuroprosthetic Devices. IEEE Transactions on Neural Systems and Rehabilitation Engineering 18(1), 67–74 (2010)

25. Schiele, A., van der Helm, F.C.T.: Kinematic Design to Improve Ergonomics in Human Machine Interaction. IEEE Transactions on Neural Systems and Rehabilitation Engineering 14(4), 456–469 (2006)
26. Kim, H., Miller, L.M., Byl, N., Abrams, G.M., Rosen, J.: Redundancy Resolution of the Human Arm and an Upper Limb Exoskeleton. IEEE Transactions on Biomedical Engineering 59(6), 1770–1779 (2012)
27. Jarrassé, N., Morel, G.: Connecting a Human Limb to an Exoskeleton. IEEE Transactions on Robotics 28(3), 697–709 (2012)
28. van den Bogert, A.J.: Exotendons for assistance of human locomotion. Biomedical Engineering Online 2(17) (2003)
29. Kobayashi, H., Hiramatsu, K.: Development of Muscle Suit for Upper Limb. In: IEEE International Conference on Robotics and Automation (ICRA), New Orleans, LA, USA, pp. 2480–2485 (2004)
30. Xu, K., Qiu, D., Simaan, N.: A Pilot Investigation of Continuum Robots as a Design Alternative for Upper Extremity Exoskeletons. In: IEEE International Conference on Robotics and Biomimetics (ROBIO), Phuket, Thailand, pp. 656–662 (2011)
31. Xu, K., Qiu, D.: Experimental Design Verification of a Compliant Shoulder Exoskeleton. In: IEEE International Conference on Robotics and Automation (ICRA), Karlsruhe, Germany (accepted for presentation, 2013)
32. Xu, K., Zhao, J., Qiu, D., Wang, Y.: A Pilot Investigation of a Continuum Shoulder Exoskeleton for Anatomy Adaptive Assistances. IEEE Transactions on Robotics (2013)
33. Xu, K., Simaan, N.: An Investigation of the Intrinsic Force Sensing Capabilities of Continuum Robots. IEEE Transactions on Robotics 24(3), 576–587 (2008)
34. Simaan, N., Xu, K., Kapoor, A., Wei, W., Kazanzides, P., Flint, P., Taylor, R.H.: Design and Integration of a Telerobotic System for Minimally Invasive Surgery of the Throat. International Journal of Robotics Research 28(9), 1134–1153 (2009)
35. Ding, J., Goldman, R.E., Xu, K., Allen, P.K., Fowler, D.L., Simaan, N.: Design and Coordination Kinematics of an Insertable Robotic Effectors Platform for Single-Port Access Surgery. IEEE/ASME Transactions on Mechatronics, Early Access Articles (2012)
36. Xu, K., Goldman, R.E., Ding, J., Allen, P.K., Fowler, D.L., Simaan, N.: System Design of an Insertable Robotic Effector Platform for Single Port Access (SPA) Surgery. In: IEEE/RSJ International Conference on Intelligent Robots and Systems (IROS), St. Louis, MO, USA, pp. 5546–5552 (2009)
37. Xu, K., Simaan, N.: Analytic Formulation for the Kinematics, Statics and Shape Restoration of Multibackbone Continuum Robots via Elliptic Integrals. Journal of Mechanisms and Robotics 2 (2010)